Numerical Study of Heat Transfer Characteristics of Turbulent Iso-Thermal Jet Impinging On a Flat Surface

T.Muneiah[1] E.Bhaskar [2] Ch.Venkata Rajesh[3]
[1, 2, 3] Assistant professor, Department Of Mechanical Engineering
[1, 2] Priyadarshini college of engineering & Technology, Kanuparthipadu, SPSR Nellore-4.
[3]Bahamiah College of Engineering, SPSR.Nellore-524366

Abstract— In this paper four turbulent models and two methods to account for the wall effect on the flow and heat transfer are tested for their predictive capabilities in impinging flows. The models are the $k - \varepsilon$ STD, $k - \varepsilon$ RNG, $k - \omega$ SST and v2f model with integration to the wall. First a description of the models is given and some results for a generic test case are presented to highlight some of the characteristics of the different models.

Next from these models selected the best one which gives the requirement are used to calculate the flow and heat transfer of a single impinging jet. Originally, most turbulent models were developed for attached flows along flat or mildly curved walls. The impinging jet flow has a different characteristic, i.e. a flow that changes direction from a wall-normal one to a wall-parallel one. Therefore the single impinging jet provides a different and challenging test case for the performance of turbulence models. The results indicate good prediction of the flow by second moment closure models. The best results for heat transfer are obtained with the models using integration to the wall. Numerical results are compared with experimental data, for the heat transfer. The results show the good prediction of the Blending Model for the flow and heat transfer.

Keywords: - Numerical Study; Heat Transfer Characteristics; Turbulent Iso-thermal; Flat surface;

I. INTRODUCTION

Impingement heat transfer is considered as a promising heat transfer enhancement technique. Among all convection heat transfer enhancement methods, it provides significantly high local heat transfer coefficient. At the surface where a large amount of heat is to be removed /addition, this technique can be employed directly through very simple design involving a plenum chamber and orifices.

Impinging jets contain several flow regimes, which make the flow interesting for studying turbulence and heat-transfer physics. The most common impinging jets are divided into three distinctive regions: the free-jet zone, the stagnation region and the wall-jet region. In the free-jet zone, the issuing jet starts to interact with the ambient fluid. Instabilities of the Kelvin-Helmholtz type occur in the newly formed shear layer. The growth of instabilities leads to formation of ring vortices The free-jet region can be divided, additionally, into three subregions: the jet core, the developing-zone and the fully-developed zone. The jet core is the central region in which the velocity remains equal to the nozzle-exit velocity. If the jet issues from a stagnant or slowly moving non-turbulent flow through a well-shaped nozzle, the flow in the core is inviscid and the jet core is called the potential core. If the free-jet region is sufficiently long (H/D > 6), the jet core starts to break down due to a strong mixing in the shear layer. The existence of the jet core, especially if it is shear-stress-free at the moment when the jet impacts the wall, has a profound effect on the shape of the Nusselt-number distribution. In the developing zone, the axial velocity starts to decay as a result of the strong shear in the jet boundary. Entrainment is additionally enhanced, which leads to a fully developed velocity profile.

As the jet approaches the wall, the impermeability condition begins to affect the velocity and stress fields. A stagnation region is formed in the centre of the impingement zone. The axial velocity reduces; follow by the decrease of the axial momentum and the turbulent normal-stress and the increase of the static pressure. The positive contribution of the turbulent normal stresses in the axial momentum equation, in the wall vicinity, means that a part of energy from the turbulent field is transported back into the mean velocity field. The negative production of turbulent kinetic energy in the stagnation region, close to the wall, was confirmed both by experiments and numerical results.

On the other hand, few results of computer simulations of the impinging jets at higher Reynolds numbers can be found in literature. The reported studies covered either the plane (slot) jets, which pose significantly less computational challenge than round jets (no radial spreading of the wall-jet), or the round jets at low Reynolds numbers. In several studies published, external forcing was imposed to facilitate the creation of stronger coherent structures, thus making the simulations more effective.

II. LITERATURE REVIEW

Gardon and Akfirat (1965) studied the role of turbulence in explaining the heat transfer phenomena in impinging jet. Hoogendoorn (1977) investigated the effect of turbulence on the stagnation heat transfer from a flat surface into an impinging jet. He employed liquid crystal techniques and concluded that the increase in the stagnation point Nusselt number is similar to the increase for the stagnation point on a cylinder in a free stream. At low turbulence levels and for smaller nozzle exit to plate spacings, the Nusselt number at the stagnation point was less than a point directly around it.

Priedeman et al. (1994) used extended surfaces with an impinging liquid jet and compared his results to a smooth reference surface. The ratio of the modified surface area to the smooth surface area range from 1.6 to 4.8. They found that the average Nusselt number increase or decrease above the corresponding values for the smooth surface depending on the surface configuration. This can be explained by the balance between the momentum decay to the extended surfaces and the increase in turbulent intensity. Sullivan et al. (1992) used smooth and rough spreading plates to enhance the heat transfer between a circular liquid jet and a small heat transfer. They found that heat transfer increases with the roughness spreader plates and increasing

nozzle diameter. They speculated that surface roughness enhances that heat transfer by increasing turbulence in the boundary layer.

Baughn and Shimizu (1989) have investigated the heat transfer characteristics of a single circular turbulent air jet issuing from a long pipe and impinging on a flat stationary surface. They studied the effect of the nozzle-to-plate distance on the radial profiles of the Nusselt number. Results for a jet with a Reynolds number of 23,750 were conducted. The Nusselt number (N_u) on the impingement plate is plotted as a function of the radial distance from the stagnation point of the jet (R/D) at four nozzle-to-plate distances (H/D). In general, the Nusselt number is highest in the stagnation point of the jet, for all values of H/D, and gradually decreases with increasing radial distance. This is caused by the growth of the thermal boundary layer in the wall jet and the decrease of wall jet velocity with increasing radial distance.

Shi et al. (2002) present computational fluid dynamics model results for heat transfer under a semi-confined slot turbulent jet under thermal boundary conditions such that the temperature-dependence of the fluid properties affects the flow and thermal fields. A comparative analysis in the turbulent flow regimes is made of the standard k-ε and Reynolds stress turbulence models for constant target surface temperature. Results show that large temperature differences between the jet and the impingement surface lead to significant difference in the heat transfer coefficients. Small temperature difference (e.g., up to 50^{o}C) show only minor differences between the local Nusselt number calculated using thermal conductivity values at the jet, film or wall temperature. Large temperature differences (over 100^{o}C) can result insignificant differences between the three possible definitions of the Nusselt number. This is true for both heating and cooling with impinging jets. It is shown that use of the jet temperature as the reference temperature for the calculation of the Nusselt number shows the least spread. Empirical correlations are provided for the average and stagnation Nusselt number under a semi-confined turbulent slot jet based on the numerical results.

Liakos et al. (2004) conducted a numerical modeling of jet impingement cooling onto a semicircular concave surface. The performance of two-equation turbulence models k-ε is evaluated vs. the Reynolds stress model. They concluded satisfying agreement numerical predictions and experiments could be achieved with the combination of an unstructured grid and any of the two turbulent models tested. For both models, discrepancies between experiments and predictions increase, as the nozzle-to-target distance is decreased from 10 to 4 nozzle slot jet widths. The variation of the Reynolds number had no significant influence on the predictions. Accurate predictions of the wall boundary characteristics improve calculations with both models, away from the stagnation point and in the circumferential direction. The maximum heat transfer occurred at the higher Reynolds number, attributed to turbulence level augmentation. For the same Reynolds number maximum heat transfer occur at H/D = 6.

Woei et al. (2006) studied experimental and examines the detailed heat transfer distributions over a convex dimpled surface subject to impinging jet-array of three sets. The isolated and combined effects of eccentricity between centers of jet and convex-dimple, Reynolds-number and separation-distance on local heat transfers over the impinging dimpled-surface are investigated. Heat transfer augmentations generated by the convex dimpled surface over the smooth-walled counterpart for various test scenarios are unraveled with the attempt to identify the operating conditions that signify the considerable heat transfer enhancements. The jet-to-dimple eccentricity has demonstrated the considerable impacts on the local and area-averaged heat transfers due to its effects on the inter-jet reactions, which involve the modified jet momentum and wall-jet flows. Heat transfer enhancements relative to the smooth-walled levels are about 10-30% of Nu_∞ levels. The peak ratios of Nu / Nu_∞ value develop at the separation distance of 0.5 D_j for all three jet-to-dimple eccentricities tested. The jet-array assembly with eccentricity provides the relatively high Nusselt number ratios that are suggested for cooling applications of combustion chamber of gas turbine engine when the impinging jet-array system with convex dimpled surface is employed.

Zhou and Lee (2006) did experimental investigation and studied on fluid flow and heat transfer characteristics of a rectangular air jet with sharp edge rectangular nozzle impinging on a heated flat plate. Both concluded that effects of jet Reynolds number and nozzle-to-plate spacing on local and average Nusselt number have a significant influence on heat transfer behaviors of impinging jets, especially on the impingement region. The results indicate that, as the aspect ratio increases, the speed of mixing in the very near flow field increases while the potential core length decreases. The axial and lateral heat transfer data at various test conditions were correlated with a least squares fit, taking into account the effect of the turbulence intensity. The rectangular jet is now being used for thrust vectoring and enhanced mixing in the aerospace industry.

III. NUMERICAL SIMULATION

Turbulent flows are characterized by fluctuating velocity fields. These fluctuations mix transported quantities such as momentum, energy, and species concentrated, and causes the transported quantities to fluctuate as well. Since these fluctuations can be small scale and high frequency, they are too computationally expensive to simulate directly in practical engineering calculations. Instead, the instantaneous (exact) governing equitation can be time-averaged, ensemble-averaged, or otherwise manipulated to remove the scales, resulting in a modified set of equations that are computationally less expensive to solve. However, the modified equations contain additional unknown variables, and turbulence models are needed to determine these variables in terms of known equations. Here, in the present study commercial CFD code FLUENT 6.3 has been used for numerical simulation of the problem. Following turbulent models were used to simulated to jet impingement heat transfer case and finally an appropriate models was chosen which was able to simulated the problem with fairly good accuracy. The selected models are:

- k - ϵ models
- Standard k - ϵ model
- Renormalization-group (RNG) k - ϵ model

- $k - \omega$ models
- Shear-stress transport (SST) k - ω model
- $\overline{\upsilon^2} - f$ model

A. Computational Domain

Figure 1 shows the symmetric computational domain used for simulation. As the problem is axi-symmetric only half portion of the domain was selected for the simulation purpose.

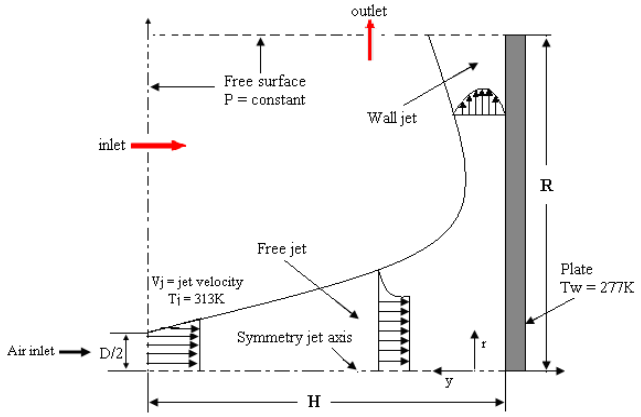

Fig. 1: Geometry of the computational domain.

The flow is axi-symmetric and incompressible with constant physical properties. The viscous dissipation is neglected. A constant temperature condition is applied to the impinge plate (no-slip is considered for velocity).

B. Boundary Conditions

Boundary conditions need to be specified on all surfaces of the computational domain. Boundaries presented in this study include inflow (inlet), solid wall and axis of symmetry as shown in Figure 1.

1) Impingement surface (wall)

For the present model, along the impingement surface, non-slip boundary condition for velocities, zero value for turbulent kinetic energy, and zero gradient for energy for energy dissipation rate were used. Temperature at the plate surface was kept constant as 277 K.

2) Flow Inlet

The velocity-inlet boundary conditions imposed at the nozzle (flow inlet) are described by.

- Air was taken as the working fluid.
- At the nozzle exit Reynolds number was varied from 5000 to 30,000.
- Jet coming from the nozzle (D = 10 mm) was at 313 K.
- At this temperature, density (ρ = 1.13 kg/m^3), thermal conductivity (k = 0.0242 W/m K) and viscosity (μ = 1.91 x 10^{-5} kg /m-s) were taken.

3) Symmetric boundary (Central axis)

As round nozzle was used for this study, symmetry boundary conditions were applied along the symmetric line/ centerline (all gradient are zero).

4) Far boundary at the flow exit

Fluid leaves the impingement plate at for exit boundary and boundary condition corresponding to that was kept at constant pressure (p = p_{atm}).

5) Far boundary at the back

At the back of the domain, where the entrained fluid was coming boundary condition was also taken as constant pressure (p = p_{atm}).

C. Grid Description

Figure 2 shows the mesh domain. The grid was designed with respect to an expected flow field in the jet geometry. The grid is being given the use of symmetry in related to the jet axis to reduce number of volume elements.

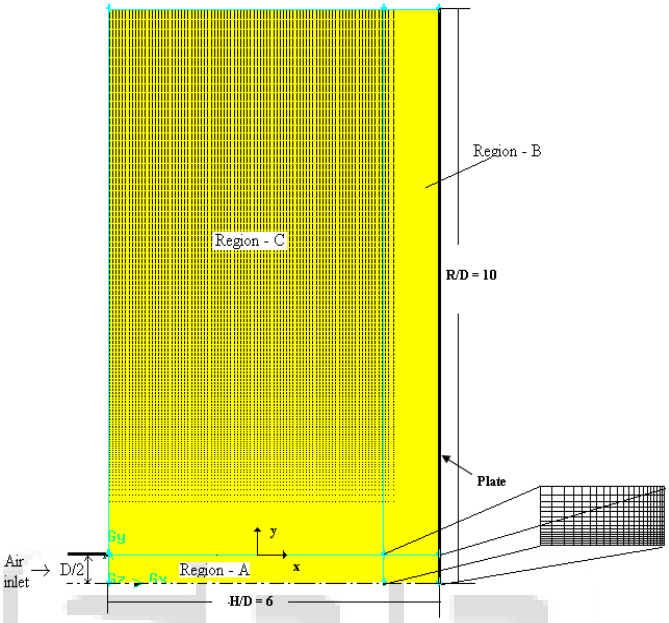

Fig. 2: Mesh domain.

Grid is composed from three grid areas, A, B, C, which are bound together. The first area, A, is located just behind the inlet; and it contains the pipe for the flow evolution. A- part of grid is designed to be structured rectangular grid with respect to laminar flow in this 5x50mm chamber. The next chamber is B, which is the near wall region with 10x100mm. The last chamber is C, which has less effect to the flow domain, and it contains cores grid compared to the other two chambers. The camber A and B are having very fine mesh, because these two are the both main regions which control nozzle enables to capture strong velocity gradients of the jet shear layer. Special care has taken while generating the grid in the respective chambers. The total number of cells (2D axisymmetric zones) and nodes were 84000 and 84591 respectively.

IV. Results And Discussion

Results and discussion comprised of validation of turbulent models, selection of the suitable model for the present work and then parametric study of turbulent isothermal jet impinging on a flat surface. Effect of variation of dimensionless separation distance (2-10) and Reynolds number (5000-30000) on heat transfer characteristics on the target surface has been investigated.

A. Results Validation

Validation was done against the experimental results of Lee and Lee (1999) for H/D = 6 and Reynolds number of 25,000. Figure 3 shows the Nusselt number distribution on the flat surface in radial direction using five turbulent models. Simulations were carried out identical conditions to

that of experiments of Lee and Lee (1999). In the experimental results, the peak was observed at stagnation point and then decreases monotonically along the radial direction. The value of Nusselt number at stagnation point was 160 in experiments, which was higher than the corresponding valued observed in simulations (100 to 140). The trend lines are almost matching and overall the simulations results show a fairly good agreement with the experimental results.

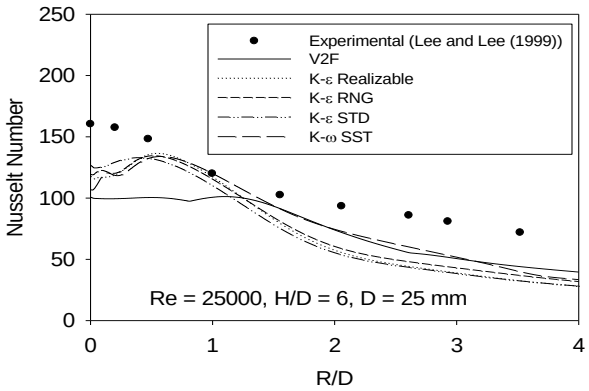

Fig. 3: Comparison of simulated and experimental results (Lee and Lee (1999)) for different turbulent models.

Table 1 shows the comparison of four different turbulent models with experimental data (Lee and Lee (1999)) at H/D = 2 and Re = 10,000 for D = 10mm. The experimental primary maximum Nusselt number was at R/D = 0.34. For numerical values $k - \omega$ SST primary Nusselt number was at R/D = 0.62, for k - ε RNG it was at R/D = 0.52 and for k - ε STD it was at R/D = 0.21. At this H/D and Reynolds number there is a secondary maximum Nusselt number in the experimental data at R/D = 1.67. In the numerical results $k - \omega$ SST and v2f models only shows secondary maximum Nusselt number at 1.68 and 2.17 respectively. No secondary maximum for $k - \varepsilon$ models. But by comparing the secondary maximum Nusselt number for $k - \omega$ SST and v2f models, the $k - \omega$ SST models gives the exact location of secondary maximum Nusselt number as in experimental data (Lee and Lee (1999)).

In v2f models the secondary maximum Nusselt number was quite far away from the stagnation point with respective to experimental data. The experimental primary maximum Nu_1 was 22.20% higher than the secondary maximum Nusselt number. In $k - \omega$ SST and v2f models there were 40.95% and 40.77% respectively. Since there was no secondary maximum in the $k - \varepsilon$ models their ratio of primary maximum Nusselt number to stagnation point Nusselt number was 0.20% and 2.8% respectively. Which is very less in their ratio and we can consider them as models with no primary maximum Nusselt numbers also. Thus these two $k - \varepsilon$ models were totally failure models when compared to the experimental values. When comparing the results of $k - \omega$ SST and v2f models, $k - \omega$ SST model was very much closer to the experimental data (Lee and Lee (1999)).

Table 1 Comparison of Nusselt number peaks for Re = 10,000, H/D = 2, D = 25 mm.

	Experimental value (Lee and Lee (!999))	$k - \omega$ SST model	V2f model	k - ε RNG model	k - ε STD model
1st peak	R/D = 0.34	R/D = 0.615	R/D = 0.54	R/D=0.52	R/D = 0.21
2nd peak	R/D = 1.67	R/D = 1.68	R/D = 2.17	-o-	-o-
	Nu_1 is 22.20% higher than Nu_2	Nu_1 is 40.95% higher than Nu_2	$Nu_1$is 40.77% higher than Nu_2	Nu_1 is 0.20% higher than Nu_0	Nu_1 is 2.8% higher than Nu_0

Figure 4 shows the variation of Nusselt number for various models of H/D = 2, at constant Reynolds number (Re = 10000) and for D = 10mm. Here, it has been observed that only two models show second maximum (secondary peak) at this separation distance i.e., the SST k-ω and the v2f model. This is in accordance with the experimental results (Lee and Lee (1999)) for this very separation distance (H/D = 2). In other two k-ε models, after the first peak, Nusselt number decreased monotonically in the radial direction. Even though, high stagnation point Nusselt numbers were observed in k-ε models still no second maximum of formed. Stagnation point Nusselt numbers were 288, 268, 259 and 233 for standard k-ε model, v2f, RNG k-ε and SST k-ω model respectively. Second maxima in Nusselt number were 155 and 148 for v2f model SST k-ω model respectively. Primary maximum in SST k-ω model was 38.4% higher than the secondary maximum. The formation of second maxima in SST k-ω was at around $1.97 \leq R/D \leq 2.2$ and for v2f model was at around $2.2 \leq R/D \leq 2.4$. The Nusselt number values at the secondary peak were about 8.5 % higher in case of SST k-ω in comparison to v2f model. After the second maxima, there was monotonically decrease in Nusselt number towards wall jet region.

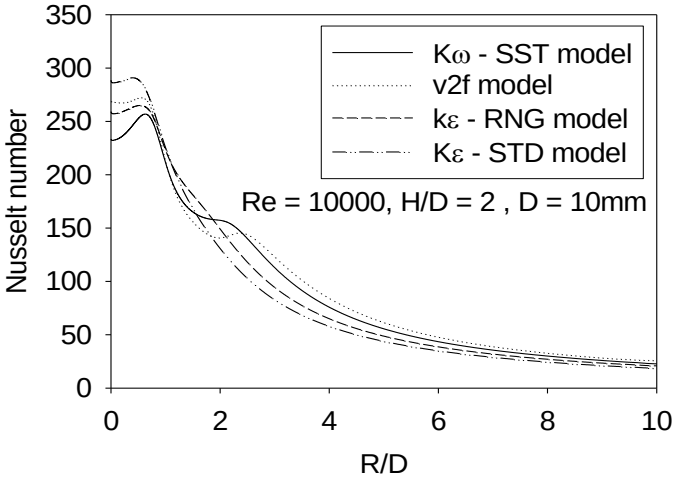

Fig. 4: Variation of Nusselt number for various models of H/D = 2, at constant Reynolds number (Re = 10000) and for D = 10 mm.

B. Effect of Reynolds Number

The local Nusselt number distributions for various Reynolds number at H/D = 2 are shown in Fig. 5. In this case, since the impingement plate is located within the

potential core length of the free jet, the corresponding heat transfer characteristics are very complicated due to the complex interaction between the impinging jet and the impingement plate. As shown in Fig. 5, the local Nusselt number increases from the stagnation point to the first peak and then decrease rapidly and again increases along the wall (for Re ≥ 10000), giving the second peak in the transition region. Moving outward from the secondary peak, Nusselt number values decrease monotonically.

The local Nusselt numbers at the first peaks are approximately 7.7% higher than the stagnation point value, and the ratio of first peak value to the stagnation point Nusselt number is found to increase with jet Reynolds number. The first peak location moves inward with increasing Reynolds number, which results from the enhanced

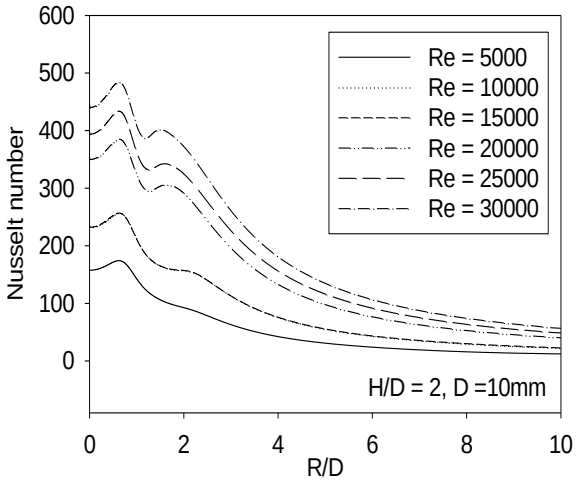

Fig. 5: Variation of Nusselt number for various values of Reynolds number at H/D = 2 and for D = 10 mm.

momentum transfer at the edge of the nozzle. On the other hand, the local Nusselt numbers at the primary maximum are approximately 16.9% higher than the secondary maximum. The primary maxima in local Nusselt number distributions corresponding to the maximum heat transfer occur at R/D of 0.62 in this study. This peak might be due to accelerating flow at low nozzle-to-plate spacing and to the local thinning of the boundary layer

The secondary maxima occur in the range 1.35 ≤ R/D ≤ 1.96 for all Reynolds number tested in this study. With increasing Reynolds number, the location of the secondary maximum also moves inward in the radial direction and the Nusselt number at the secondary maximum is increased. Martin (1977) suggested that the secondary maximum could exceed the stagnation point Nusselt number for higher Reynolds numbers, but present results show that the stagnation point heat transfer rates are always larger than the secondary maxima for all Reynolds numbers tested in this study. The formation of the secondary maxima results from the increasing momentum transport due to the transition from a laminar to a turbulent boundary layer. The present stagnation Nusselt number data for H/D = 2 are nearly 10-20% higher than those of Gardon and Akfirar (1965). These peaks were quite significant at high Reynolds number. At a Reynolds number of 5,000, the local heat transfer rates decrease monotonically from the first peak without forming the secondary peak

C. Effect of Separation Distance

It has been observed from Fig. 6 that as the nozzle-to-plate separation distance H/D (at constant Re = 5000) is increasing the inner peak curves moves radially outward, with very small change in the stagnation Nusselt number. Generally all the inner peaks are coming in the rage 0.025 ≤ R/D ≤ 0.62, which are very close to the stagnation point. Little difference is seen between the radial Nusselt number profile for nozzle-to-plate spacing of H/D = 2, 4 and 6. The only difference is, H/D = 2 shows a slight secondary peak at R/D = 2.2 whereas no such peaks is seen in the local data for the larger spacing.

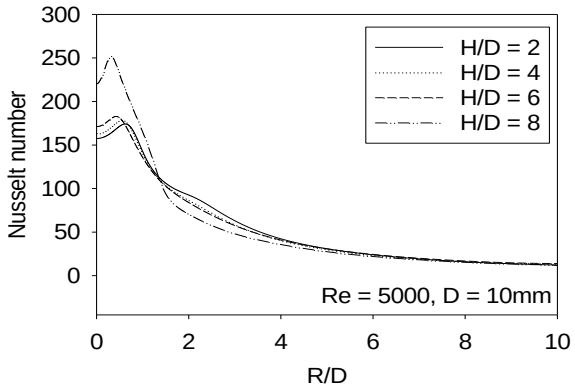

Fig. 6: Variation of Nusselt number for various values of dimensionless separation distance at constant Reynolds number (Re = 5000) and for D = 10 mm.

Vortex breakdown begins in the region of vortex–target interaction, where the flow experiences the action of an adverse pressure gradient. the impact of these large scale toroidal vortices from the jet shear layer on the velocity filed close to the impingement wall revealed that the original vortex ring break apart as it travels towards the wall. The dynamics of the toroidal vortices strongly affects the flow in the stagnation region. The velocity at the jet centerline decreases at the nozzle exit to zero on the target wall. For H/D = 8, the turbulence intensity at a distance from the nozzle exit equal to (3-4 D) is 5% higher than its value at the nozzle exit, and the turbulence intensity near the target is 25% higher than its value at the nozzle exit calculated by Volkol (2007) for the same conditions. The level of velocity fluctuations at the stagnation point remains unchanged as long as the target is in the potential core of the jet. This position depends on the value of H/D.

For high values of R/D, the distribution of heat-transfer characteristics depends on the structure of secondary vortices arising owing to interaction of the primary vortex with the boundary layer of the near-wall jet. The unsteady character of this interaction and a change in the structure of the thermal boundary layer are responsible for a local maximum in the Nusselt number. Nusselt number drops monotonically in the wall jet region. Decrease in the value of Nusselt numbers in this region is attributed to decrease in the velocities of fluid over the plate because of radial flow and excessive exchange of momentum of wall jet with surrounding air. This is due to intermittent flow separation on the impingement wall. The separation in the wall jet region is caused by the strong azimuthal rotation of large-scale toroidal vortices. These vortices originate from the jet shear layer, and after they impinge the wall they

deflect radially. The presence of the wall-attached eddies strongly affects the heat transfer and causes the non-monotonic distribution of the Nusselt number. A local dip in the Nusselt number at R/D ≈ 1.4 seems to be caused by the instantaneous local separation and the consequent thickening of the thermal boundary layer. The subsequent wall-jet re-attachment coincides with the second Nusselt number maximum. This contrasts with the conventional motion that the second maximum in the Nusselt number distribution is caused by the impingement of the jet shear layer.

Finally, the flow over the target surface forms the wall jet region. The wall jet adheres to the surface and flows over the plate interacting with the surrounding air.

V. Conclusions And Scope Of Future Work

The local heat transfer characteristics in a stagnation region were investigated numerically for an axisymmetric submerged jet impinging normal to an isothermal flat plate. In this study, numerical simulation was done using commercial computational Fluid Dynamics (CFD) code, FLUENT. Numerical results were validated with the corresponding experimental results and fairly good agreement was observed. Four turbulent models have been used. The $k - \omega$ SST showed got agreement with the published results for this kind of problems. The second peak in Nusselt number at low nozzle-to-plate distance was well predicted by only the $k - \omega$ SST model. This model has been used to evaluate the influence of nozzle-to-plate distance and Reynolds number was shown to perform well in the range of H/D and Re, in order to give confidence in its use as a predictive tool. Following major conclusions are arrived at:

(1) Numerical simulation results were fairly close to experimental results. Further $k - \omega$ (SST) showed good matching with the experimental results.
(2) Increase in Reynolds number leads to better heating due to increase in velocity and thus convective heat transfer.
(3) Decrease of nozzle-to-plate spacing would result in the increase of Nusselt number and hence heat transfer.
(4) Two peaks were observed at high values of Re and low H/D.
(5) Peaks (both primary and secondary) move towards the stagnation point when increasing Reynolds number.
(6) Peaks move outwards the stagnation when decreasing nozzle-to-plate distance.

References

[1] Abdel-Fattah, A. (2006), **"**Numerical and experimental study of turbulent impinging twin-jet flow", Department of Mechanical Power Engineering, Experimental Thermal and Fluid Science, Vol. No. 31, pp. 1061–1072.
[2] Bernard, A., Brizzi, L.E and Bousgarbie, J (2000)," A comparison of flow visualization and wall pressure measurements for a jet impinging on a plane surface", Experiments in Fluids, Springer-Verlag 2000, Vol. No.29, pp. 23-29.
[3] Chang, Shyy Woei, Jan, Yih-Jena, Yu, Ker-Wei, Hwang, Yao-Hsin and Chang, Shun-Fei, (2006), "Heat transfer of impinging jet-array over convex dimpled surface with application to cooling of combustion chamber of gas turbine engine", International Journal of Heat and Mass Transfer, Vol. No. 49, pp. 3045–3059.
[4] Chiang, K.F., Chang, S.W. and P.H. Chen (2004), "Forced convective heat transfer of 45^o rib-roughened fin flows", Department of Mechanical Engineer, Experimental Thermal and Fluid Science, Vol. No. 29, pp. 743–754.
[5] Fenot, M., Dorignac, E., and Vullierme, J. (2005), "An experimental study on hot round jets impinging a concave surface", International Journal of Thermal Sciences, Vol. No. 44, pp. 665–675.
[6] Gao Lujia (2003), "Effect of jet hole arrays arrangement on impingement heat transfer", Department of Mechanical Engineering, A. Thesis, Shanghai Jiao Tong University.
[7] Gao Lujia (2003), "Effect of jet hole arrays arrangement on impingement heat transfer", Department of Mechanical Engineering, A. Thesis, Shanghai Jiao Tong University.
[8] Gardon, R. and Cobonpue, J. (1961), "Heat transfer between a flat plate and jets of air impinging on it", ASME, Int. Development in Heat Transfer, Part 2. pp. 454-460.
[9] Gardon, R. and Akfirat, J. (1965), "The role of turbulence in determining the heat-transfer characteristics of impinging jets", Int. J. Heat Mass Transfer, Vol. No. *8*, pp. 1261-1272.
[10] Geers, L. F. G. (2003), "Multiple impinging jet arrays: an experimental study on flow and heat transfer". Ph. D. thesis, Delft University of Technology, Delft, The Netherlands.
[11] Geers, L., K. Hanjali, C and M. Tummers (2005), "Wall imprint of turbulent structures and heat transfer in multiple impinging jet arrays", J. Fluid Mech. - accepted for publication.
[12] Goldstein, R.J., and Behbahani, A.I., and Heppelmann, K.K. (1986), "Stream wise distribution of the recovery factor and the local heat transfer coefficient to an impinging circular air jet," International Journal of Heat and Mass Transfer, Vol. 29, pp. 1227-1235.
[13] Hoogendoorn, C. J. (1975), "The effect of turbine on heat transfer at a large scale eddies", Proc. 9th Int. Heat transfer Conf., Vol. No. 18, pp. 597-605.
[14] Jung-Yang San and Wen-Zheng Shiao (2006), "Effects of jet plate size and plate spacing on the stagnation Nusselt number for a confined circular air jet impinging on a flat surface", Department of Mechanical Engineering, International Journal of Heat and Mass Transfer, Vol. No. 49, pp. 3477–3486.
[15] Koopman, R. N. and E. M. Sparrow (1976), "Local and average transfer coefficients due to an impinging row of jets", Intl. J. Heat Muss Transfer, Vol. No.19, pp.6733-6872.
[16] Lee, D., Grief, R. and Lee, S. J. (1995), "Heat transfer from a flat plate to a filly developed axisymmetric impinging jet", ASME J. Heat Transfer, Vol. No. 117, pp. 772-776.
[17] Lytle, D. and B. W. Webb (1991), "Secondary heat transfer maxima for air jet impingement at low nozzle-to-plate spacing", In J. F. Keffer, R. K. Shah, and E. N. Ganic (Eds.), Experimental Heat Transfer, Fluid Mechanics and Thermodynamics. Elsvier, New York.

[18] Lytle, D. and B. Webb (1994), "Air jet impingement heat transfer at low nozzle-plate spacings", Int. J. Heat Mass Transfer, Vol. No. 37, pp. 1687-1697.
[19] Murray, B., Colin Glynn and Darina (2005), "Jet impingement cooling in micro scale", Department of Mechanical and Manufacturing Engineering, ECI International Conference on Heat Transfer and Fluid Flow in Micro scale, Castelvecchio Pascoli.
[20] Murray, D. B., O'Donovan, T. S. (2005), "Effect of vortices on jet impingement heat transfer", Dept of Mechanical & Manufacturing Engineering, University of Dublin Trinity College Dublin, Ireland.
[21] Osama M. and Al-aqal A. (2003), "Heat transfer distribution on the walls of a narrow channel with jet impingement and cross flow", School of engineering, Ph. D. thesis, University of Pittsburgh.
[22] Puneet Gulati, Vadiraj Katti and Prabhu,S. V. (2009),"Influence of the shape of the nozzle on local heat transfer distribution between smooth flat surface and impinging air jet", Department of Mechanical Engineering, International Journal of Thermal Sciences, Vol. No. 48, pp. 602–617.
[23] Sagot, B., Antonini, G., Christgena, A., Burona F. (2008), "Jet impingement heat transfer on a flat plate at a constant wall temperature" International Journal of Thermal Sciences, Vol. No. 47, pp. 1610–1619.
[24] Volkov, K. N. (2006), " Interaction of a circular turbulent jet with a flat target", Journal of Applied Mechanics and Technical Physics, Vol. 48, No. 1, pp. 44–54.
[25] Xianchang Li, J. Leo Gaddis, Ting Wang and Xianchang Li (2003), "Mist/Steam heat transfer with jet impingement onto a concave surface", Department of Mechanical Engineering, ASME, Vol. No. 125, pp.438-446.
[26] Zhou D.W. and Sang-Joon Lee (2006), "Forced convective heat transfer with impinging rectangular jets", Department of Mechanical Engineering,

